Supplemental information

for

Prototropic Equilibria in DNA containing One-electron Oxidized GC: Intra-duplex and Duplex-solvent Deprotonation

by

Amitava Adhikary, Anil Kumar, Shawn A. Munafo, Deepti Kahnduri, and Michael D. Sevilla *

Department of Chemistry
Oakland University
Rochester, MI 38309

Supplemental information:

Figure S1   Fits used to estimate error limits of our Simulations of the experimentally obtained ESR spectra

Figure S2   ESR spectra of the guanine cation radical (G•$^{+}$) from 1-Me-Guo and dGuo.

Figure S3   ESR spectra of the guanine cation radical (G•$^{+}$) from 1-Me-Guo and Guo.

Figure S4   ESR Spectra of the one-electron oxidized 1-Me-Guo and 1-Me-dGuo.

Figure S5   Comparison of the ESR spectrum 1-Me-dG(N2-H)• in 7.5 M LiCl/H_2O with that of 1-Me-dG(N2-H)• in 15 M LiCl/H_2O.

Figure S6   Renaturation curve of the ds DNA oligomer in 7.5 M LiCl/H_2O

Figure S7   ESR Spectra of the one-electron oxidized ds DNA-oligomers.

Figure S8   Sugar radical formation via photo-excitation of G(N1-H)•:C(+H^{+}) and G(N2-H)•:C formed in the ds DNA oligomer

Table T1   Compilation of the already reported experimental (ESR/ENDOR studies of X-ray irradiated single crystals) and theoretical HFCC values for the N2-deprotonated neutral radical (G(N2-H)•).

Complete Reference of Reference no. 37.
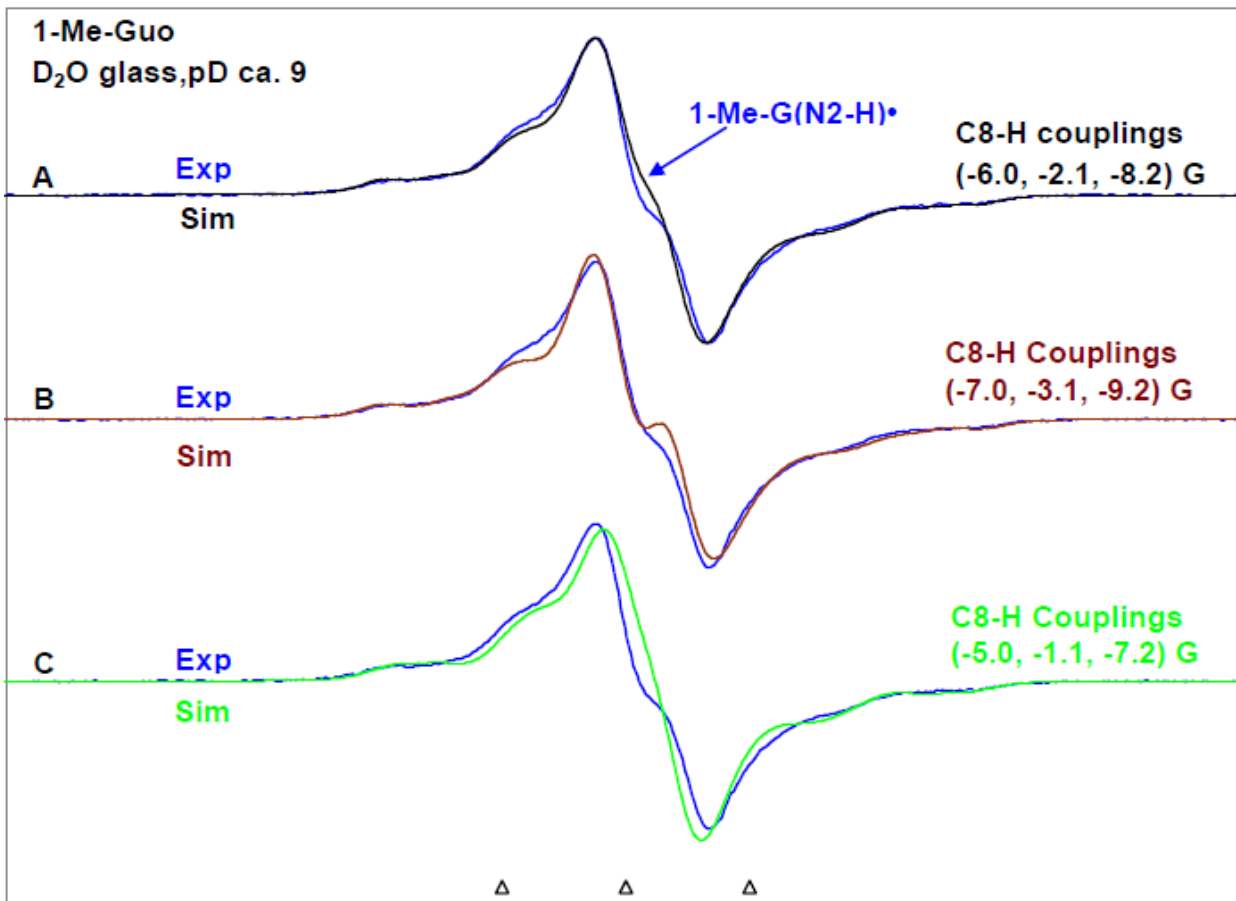
Figure S1. Fits used to estimate error limits of our simulations of ±1G for the three C8-H couplings taking the ESR spectrum (blue) of 1-Me-G(N2-H)• in 1-Me-Guo (pD ca. 8.5 to 9) as an example. The simulation parameters are described below. A. (Black) Best fit couplings. B. (Brown) Best fit +1 G. C. (Green) Best fit -1 G.

Color - simulated spectrum (with different C8-H couplings)
Blue color - experimentally obtained spectrum
Blue, brown, and green colored spectra are the simulated ones obtained using the theoretical parameters.
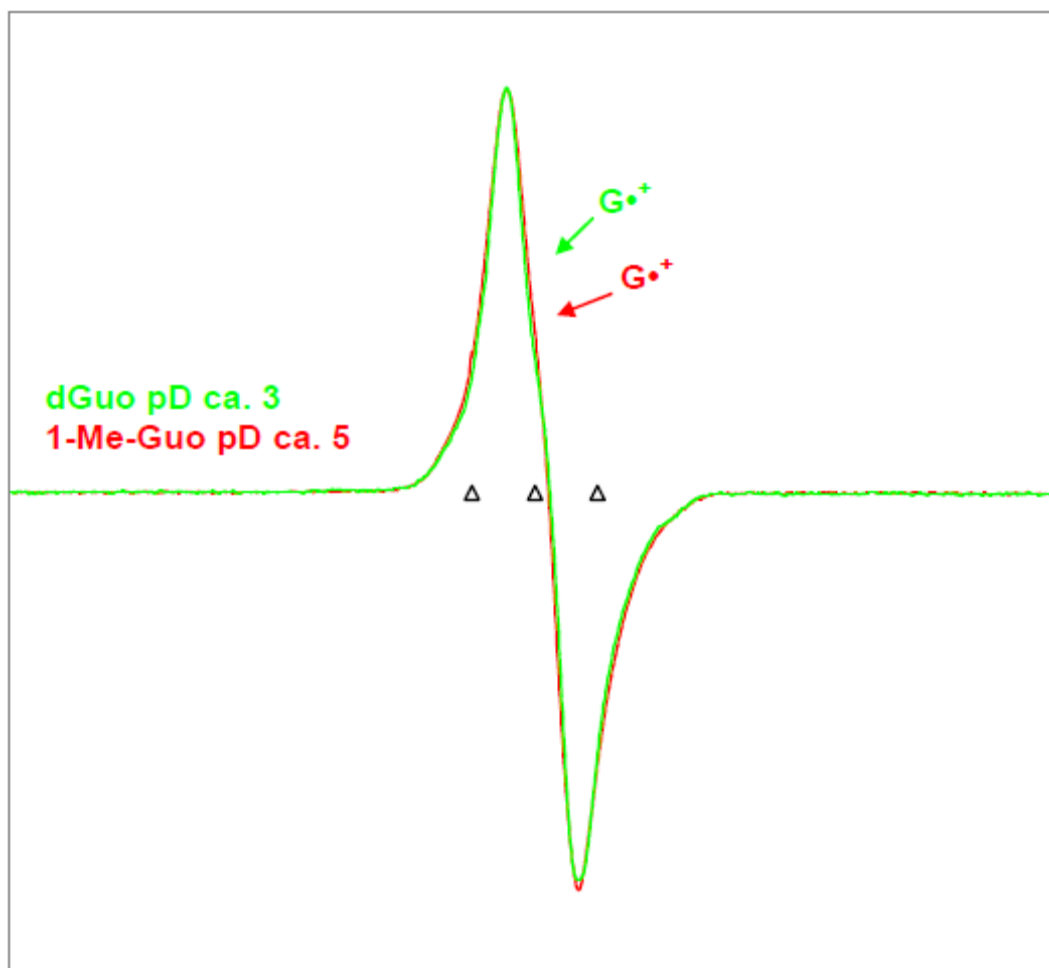
Simulation parameters which are kept constant:
N3 (12.5, 0, 0) G, N2 (15.7, 0, 0) G
g (2.0019, 2.0041, 2.0041)
Line-width (4.8, 5.7, 5.5) G
Lorentzian/Gaussian =0.8

Figure S2. ESR spectrum (green color) of the guanine cation radical ($G\bullet^+$) formed by $Cl_2\bullet^-$ oxidation of dGuo (3 mg/mL) in a homogeneous glassy (7.5 M LiCl in D_2O) solution at pD *ca.* 3 via thermal annealing at $150 - 155$ K in the dark (see Figure 2 in ref. 21). ESR spectrum (red) of the one-electron oxidized 1-Me-Guo produced by $Cl_2\bullet^-$ oxidation of 1-Me-Guo (3 mg/mL) at the native pD *ca.* 5 in a homogeneous glassy (7.5 M LiCl in D_2O) solution via thermal annealing at $150 - 155$ K in the dark. Both spectra were recorded at 77 K. The very close similarities in overall hyperfine splitting, anisotropic nitrogen hyperfine couplings, lineshape, and the center of these two spectra show they are for the same radical and establish that the one-electron oxidized 1-Me-Guo is from $G\bullet^+$.
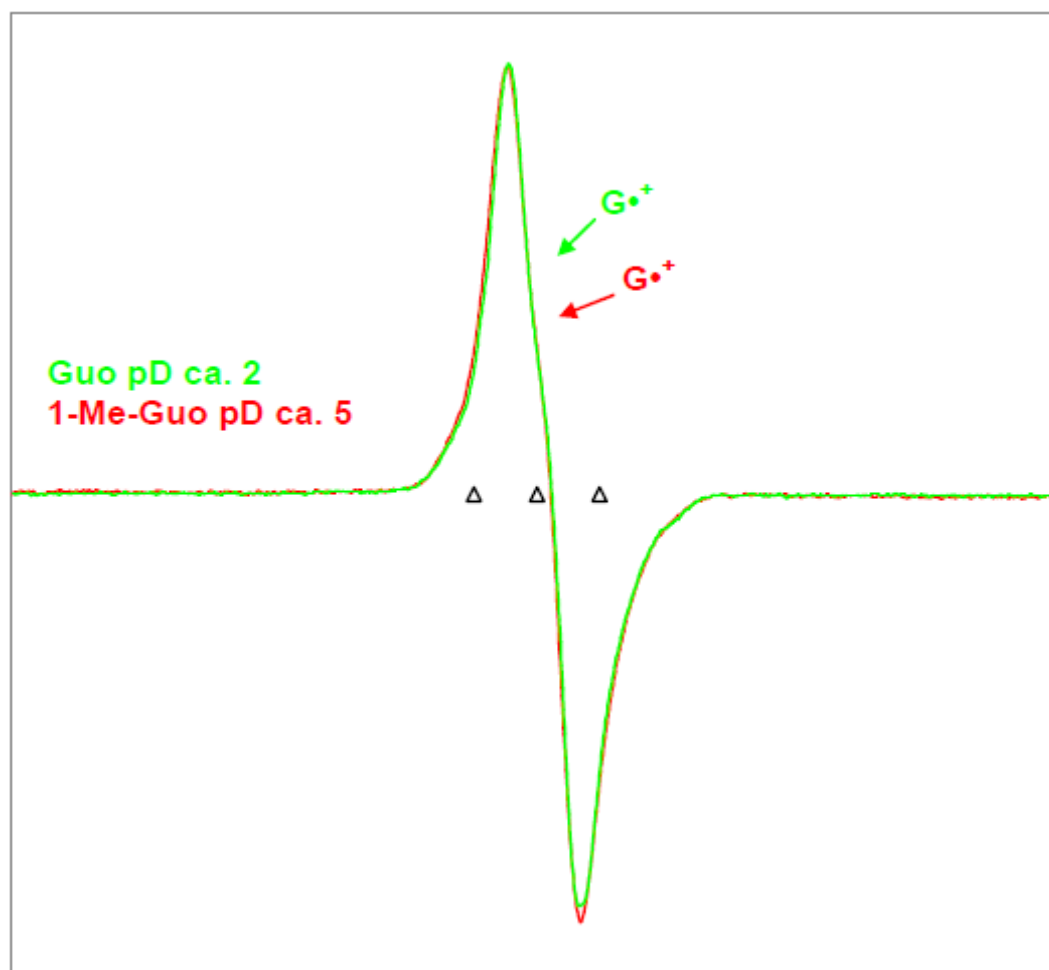
Figure S3. ESR spectrum (green color) of the guanine cation radical ($G\bullet^+$) formed by $Cl_2\bullet^-$ oxidation of Guo (3 mg/mL) in a homogeneous glassy (7.5 M LiCl in D_2O) solution at pD *ca.* 2 via thermal annealing at 150 – 155 K in the dark (see Figure 3 in ref. 27). ESR spectrum (red) of the one-electron oxidized 1-Me-Guo produced by $Cl_2\bullet^-$ oxidation of 1-Me-Guo (3 mg/mL) at the native pD *ca.* 5 in a homogeneous glassy (7.5 M LiCl in D_2O) solution via thermal annealing at 150 – 155 K in the dark. Both spectra were recorded at 77 K. The very close similarities in overall hyperfine splitting, anisotropic nitrogen hyperfine couplings, lineshape, and the center of these two spectra show they are for the same radical, and again establish that the one-electron oxidized 1-Me-Guo is from $G\bullet^+$.
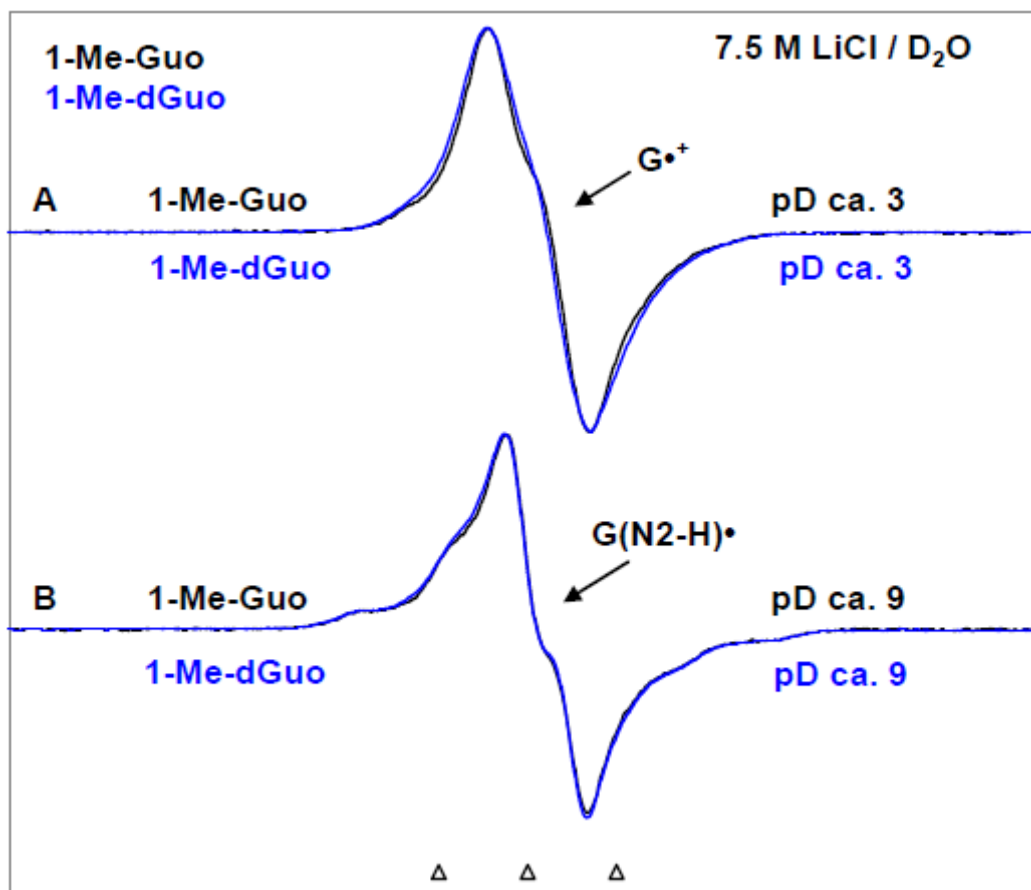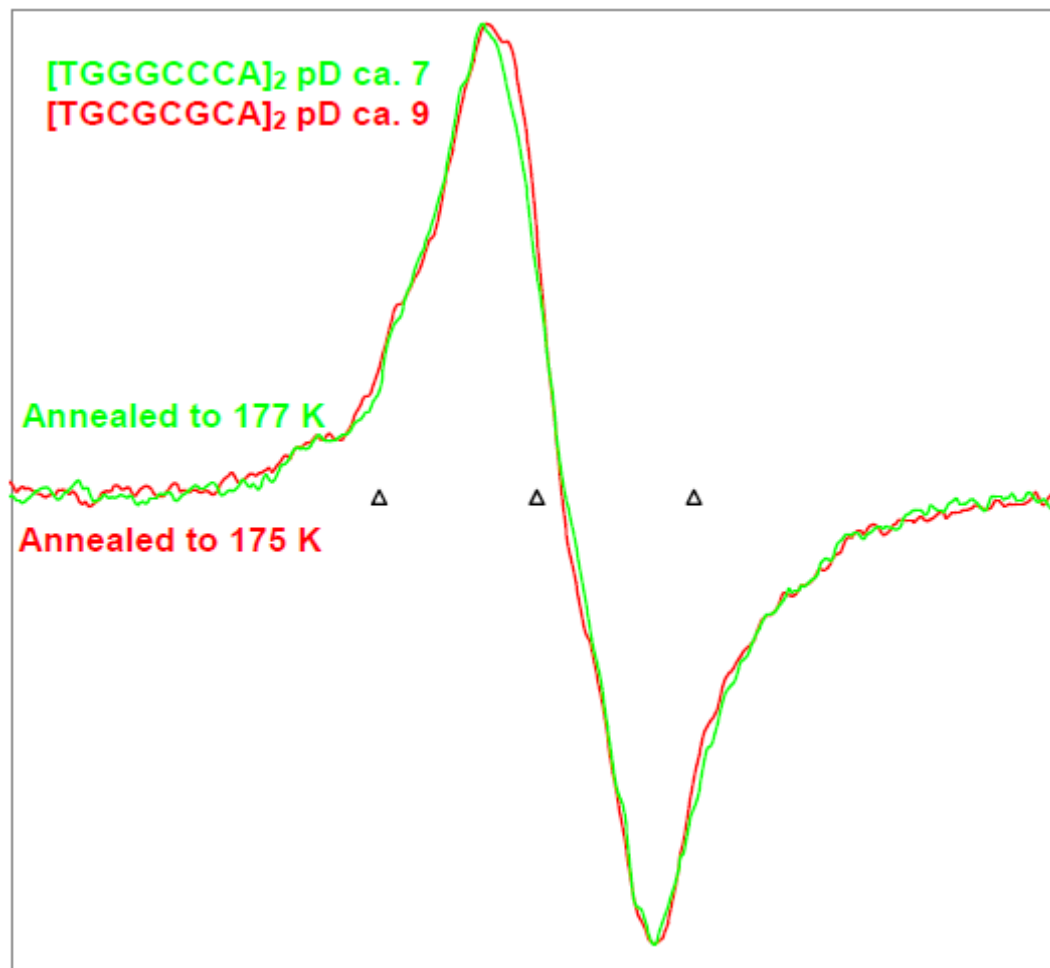
Figure S4. ESR Spectra of the one-electron oxidized 1-Me-Guo (black) and 1-Me-dGuo (blue). One-electron oxidation of each compund (3 mg/mL) was caused by $Cl_2^{•-}$ at pD ca. 3 and at ca. 9 in the homogeneous glassy (7.5 M LiCl in D_2O) solution via thermal annealing at $150 - 155$ K in the dark. All spectra were recorded at 77 K. The ESR spectra in A and B show that the cation radical ($G•^+$), and the deprotonated cation radical G(-H)• are identical for 1-Me-Guo (black) and 1-Me-dGuo (blue). Our results show that, for one-electron oxidized 1-Me-Guo, and 1-Me-dGuo, $G•^+$ is found at pDs ≤ 5, and G(N2-H)• is found at pD $7.5 - 12$. These results are in complete agreement with the UV-vis spectral results shown in Figure 1.
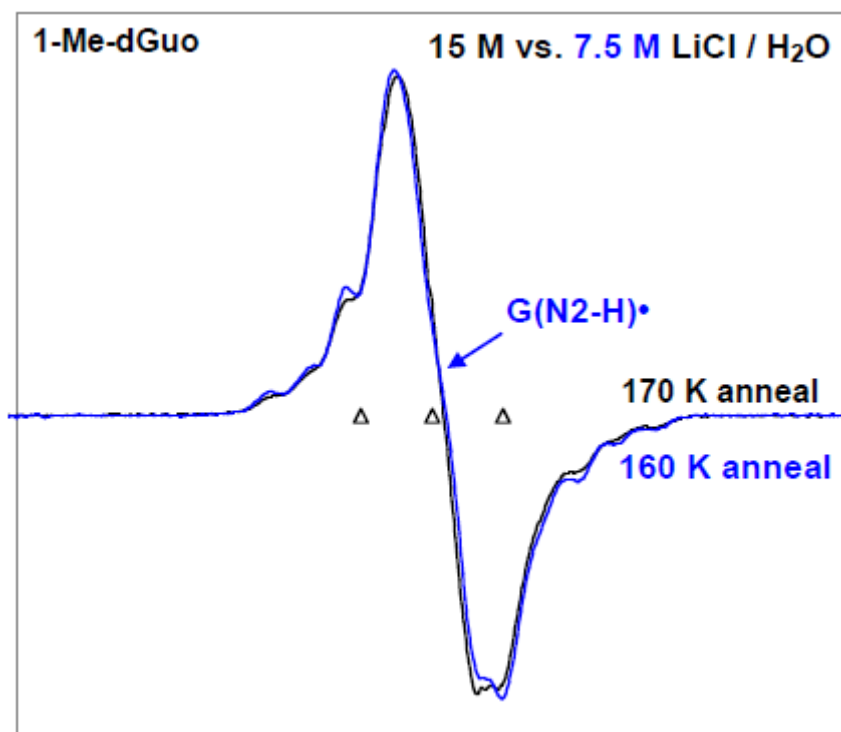
Figure S5. ESR spectra for one-electron oxidized 1-Me-dGuo (black) at pH ca. 9 (3 mg/mL) in 15 M LiCl glasses in H_2O. The black colored spectrum shown here is the spectrum of 1-Me-G(N2-H)• recorded at 77 K after its production by annealing to 170 K for 15 min in the dark. The authentic spectrum of G(N2-H)• (blue) obtained by one-electron oxidation of 1-Me-dGuo at pH 9 in 7.5 M LiCl/ H_2O glass is superimposed on spectrum B for comparison. All ESR spectra were recorded at 77 K. These results show that increase in LiCl concentration from 7.5 M to 15 M does not have any observable effect on the prototropic equilibrium of 1-Me-G(N2-H)• in 1-Me-dGuo or in 1-Me-Guo.
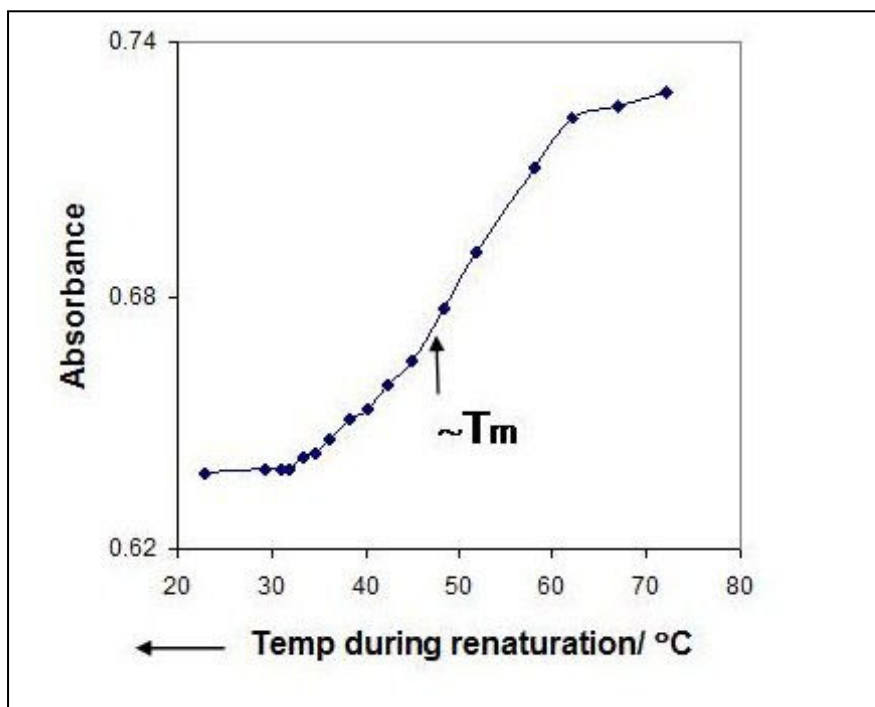
Figure S6. The renaturation curve of d[TGCGCGCA]$_2$ in 7.5 M LiCl/H$_2$O based on the absorbance at 274 nm .

Figure S7. ESR Spectra of the one-electron oxidized d[TGGGCCCA]$_2$ (green) and d[TGCGCGCA]$_2$ (red). One-electron oxidation of each oligomer (1.5 mg/mL) was caused by Cl$_2$•$^-$ at pD *ca.* 9 for d[TGCGCGCA]$_2$ and at pD ca. 7 for d[TGGGCCCA]$_2$ in the homogeneous glassy (7.5 M LiCl in D$_2$O) solution via thermal annealing at 175 – 177 K in the dark. All spectra were recorded at 77 K.
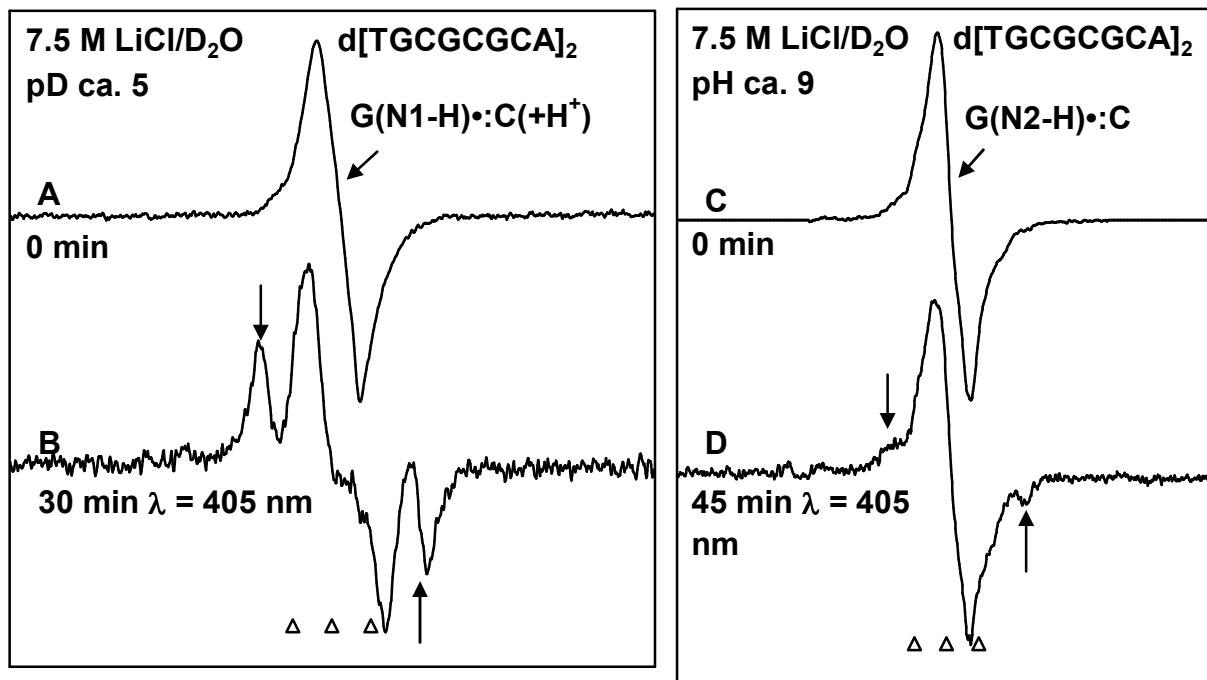
Figure S8. (A) and (C) ESR spectra of one-electron oxidized d[TGCGCGCA]$_2$ in 7.5 M LiCl/D$_2$O in the presence of K$_2$S$_2$O$_8$ as an electron scavenger at two pHs - at pH ca. 5, and at ca. 9. Spectrum (A) is assigned to G(N1-H)•:C(+H$^+$) (see Figure 4 and its relevant discussion in the manuscript); whereas, spectrum (C) is assigned to G(N2-H)•:C(see Figure 4 and its relevant discussion in the manuscript).

   After (B) 30 min, and (D) after 45 min of photo-excitation by a 405 nm laser (20 mW) at 148 K, sugar radical formation indicated by the arrows is shown in Figure (B). The outer components are due to the C1'-radical. The extent of sugar radical formation via photo-excitation of one-electron oxidized d[TGCGCGCA]$_2$ at pH ca. 5 is found to be near complete (ca. 90%) whereas the corresponding extent of sugar radical formation at pH ca. 9 for a longer irradiation is minor (ca. 20%). All spectra were recorded at 77 K.

Table T1. Compilation of the already reported experimental (ESR/ENDOR studies of X-ray irradiated single crystals[40]) and theoretical (DFT/B3LYP/6-31G(d)) [41a] HFCC values for the N2-deprotonated neutral radical (G(N2-H)•)

Method	Molecule	Atom	HFCC values (G) ($A_{ii} = A_{iso} + T_{ii}$)			
			A_{iso}	T_{zz}	T_{yy}	T_{xx}
Experimental		N2-H	-9.5	-0.9	7.7	-6.9
	5'-dGMP [40 l]	C8-H	-5.0	-0.1	2.6	-2.5
	3',5'-cyclic Guanosine 5'-monophosphate [40 j]	N2-H	-9.5	-1.0	7.9	-6.9
ESR/ENDOR studies of X-ray irradiated single crystals		C8-H	-4.7	-0.2	2.7	-2.4
	5'-dGMP,4 H$_2$O[40 b]	N2-H	-9.6	-0.9	7.8	-6.9
		C8-H	-4.9	-0.2	2.9	-2.6
Theoretical	Guanine[41a]	N2-H	-7.6	-1.2	7.7	-6.6
		C8-H	-6.0	-0.3	3.7	-3.4
	dGuo + 7 H$_2$O [21]	N1	0.34	1.78	-0.85	-0.33
DFT/B3LYP/6-31G(d)		N2	6.47	11.16	-5.57	-5.6
		N3	5.69	9.34	-4.63	-4.67
		N7	0.0	0.63	-0.29	-0.34
		C8-H	-5.9	-0.66	3.59	-2.93

Complete reference of the reference no. 37 in the text:

30. Frisch, M. J.; Trucks, G. W.; Schlegel, H. B.; Scuseria, G. E.; Robb, M. A.; Cheeseman, J. R.; Montgomery, J. A., Jr.; Vreven, T.; Kudin, K. N.; Burant, J. C.; Millam, J. M.; Iyengar, S. S.; Tomasi, J.; Barone, V.; Mennucci, B.; Cossi, M.; Scalmani, G.; Rega, N.; Petersson, G. A.; Nakatsuji, H.; Hada, M.; Ehara, M.; Toyota, K.; Fukuda, R.; Hasegawa, J.; Ishida, M.; Nakajima, T.; Honda, Y.; Kitao, O.; Nakai, H.; Klene, M.; Li, X.; Knox, J. E.; Hratchian, H. P.; Cross, J. B.; Adamo, C.; Jaramillo, J.; Gomperts, R.; Stratmann, R. E.; Yazyev, O.; Austin, A. J.; Cammi, R.; Pomelli, C.; Ochterski, J. W.; Ayala, P. Y.; Morokuma, K.; Voth, G. A.; Salvador, P.; Dannenberg, J. J.; Zakrzewski, V. G.; Dapprich, S.; Daniels, A. D.; Strain, M. C.; Farkas, O.; Malick, D. K.; Rabuck, A. D.; Raghavachari, K.; Foresman, J. B.; Ortiz, J. V.; Cui, Q.; Baboul, A. G.;Clifford, S.; Cioslowski, J.; Stefanov, B. B.; Liu, G.; Liashenko, A.; Piskorz, P.; Komaromi, I.; Martin, R. L.; Fox, D. J.; Keith, T.; Al-Laham, M. A.; Peng, C. Y.; Nanayakkara, A.; Challacombe, M.; Gill, P. M. W.; Johnson, B.; Chen, W.; Wong, M. W.; Gonzalez, C.; Pople, J. A. Gaussian03, Revision B.04; Gaussian, Inc.: Pittsburgh, PA, 2003.